^{132}Sn + ^{96}Zr reaction: A study of fusion enhancement/hindrance

A. M. Vinodkumar,* W. Loveland, J. J. Neeway, L. Prisbrey, and P. H. Sprunger
Department of Chemistry, Oregon State University, Corvallis, Oregon 97331, USA

D. Peterson
Physics Division, Argonne National Laboratory, Argonne, Illinois 60439, USA

J. F. Liang, D. Shapira, C. J. Gross, and R. L. Varner
Physics Division, Oak Ridge National Laboratory, Oak Ridge, Tennessee 37831, USA

J. J. Kolata and A. Roberts
Department of Physics, University of Notre Dame, Notre Dame, Indiana 46556, USA

A. L. Caraley
Department of Physics, State University of New York at Oswego, Oswego, New York 13126, USA
(Received 24 June 2008; published 26 November 2008)

Capture-fission cross sections were measured for the collision of the massive nucleus ^{132}Sn with ^{96}Zr at center-of-mass energies ranging from 192.8 to 249.6 MeV in an attempt to study fusion enhancement and hindrance in this reaction involving very neutron-rich nuclei. Coincident fission fragments were detected using silicon detectors. Using angle and energy conditions, deep inelastic scattering events were separated from fission events. Coupled-channels calculations can describe the data if the surface diffuseness parameter, a, is allowed to be 1.10 fm instead of the customary 0.6 fm. The measured capture-fission cross sections agree moderately well with model calculations using the dinuclear system model. If we use this model to predict fusion barrier heights for these reactions, we find the predicted fusion hindrance, as represented by the extra push energy, is greater for the more neutron-rich system, lessening the advantage of the lower interaction barriers with neutron-rich projectiles.

DOI: 10.1103/PhysRevC.78.054608 PACS number(s): 25.70.Jj, 25.60.Pj, 25.85.−w

I. INTRODUCTION

In fusion reactions induced by neutron-rich radioactive nuclei, one expects to observe a lowering of the fusion barrier, relative to that observed in reactions induced by stable nuclei with smaller neutron to proton ratios. This is simply a geometrical effect due to the greater size of the n-rich projectile. In addition, in the synthesis of heavy nuclei with n-rich projectiles, one expects a higher survival probability of the completely fused system due to its lower fissility and the lower excitation energies.

In a series of first-generation studies of fusion induced by n-rich, intermediate mass radioactive projectiles, one has observed lower fusion barriers and enhanced fusion cross sections at a given excitation energy for the n-rich projectiles compared to similar reactions induced by stable beams with lower N/Z ratios [1–5]. For several of these systems [1,3,4], the reduced excitation functions (formed by scaling the observed cross sections by the fusion radii and the center-of-mass beam energies by the deduced fusion barriers) are the same within experimental uncertainties, indicating no new physics is involved. For two of the systems [2,5] there is evidence of a lowering of the fusion barrier and a cross section enhancement bigger than that suggested by a simple scaling. In all systems, the observed lowering of the fusion barrier is larger than that predicted by the Bass model [6] although some controversy exists for the ^{32,38}S + ^{208}Pb system [7]. In general, coupled-channels calculations are not able to reproduce the observed lowering of the fusion barriers and other explanations in terms of neutron transfer and/or flow are invoked [5,8–10].

In all of these systems, one does not generally expect significant fusion hindrance because $Z_pZ_t \leqslant 1600$. For $Z_pZ_t > 1600$, it is believed that fusion hindrance effects become prominent [11,12]. Fusion hindrance generally takes the form of an extra energy that must be supplied to the fusing system to drive it from the contact point inside the fission saddle point. This energy is loosely referred to as the "extra-push" energy although the formal definition [12] of this energy is that it is the "extra-extra push energy." Evaporation residue (ER) cross section measurements [13–22] with massive projectiles ($A \sim 100$) have clearly established the occurrence of fusion hindrance with an extra energy needed to cause fusion. This fusion hindrance was explained successfully by the extra push model developed by Swiatecki *et al.* [12,23].

Studies by Sahm *et al.* [13,14] for the $^{90-96}$Zr + ^{124}Sn reactions showed an unexpected result. As the fusing system became more neutron-rich (decreasing fissility), the fusion hindrance, as measured by the extra push energy, increased in contradiction to predictions of most theoretical models (see

* attukalv@onid.orst.edu

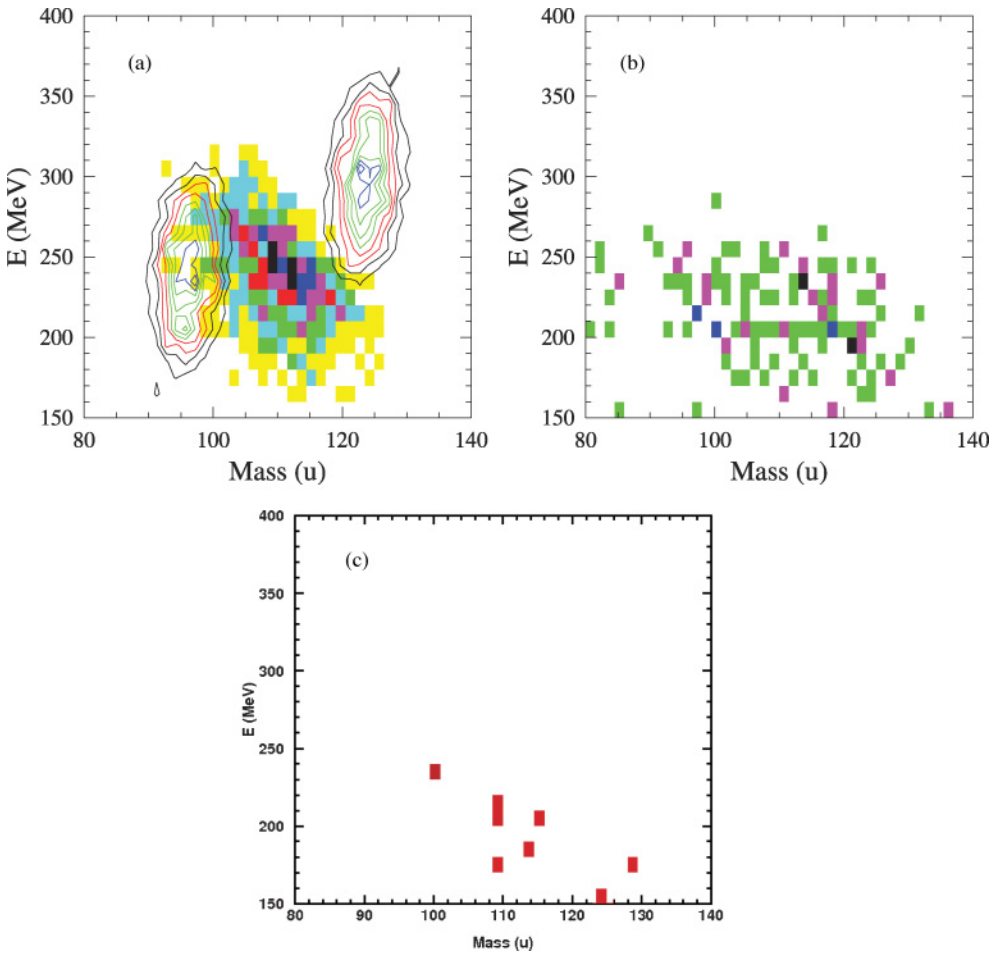

FIG. 1. (Color online) (a) Simulated coincident events for the reaction of 600 MeV ^{124}Sn with ^{96}Zr assuming the fragment detectors are at $30 \pm 10^{\circ}$. The events arising from inelastic scattering with $Q = -40$ MeV and symmetric fission are shown. (b) The same plot as (a) except the points represent the measured data for the reaction of 600 MeV ^{124}Sn with ^{96}Zr with gates applied to isolate the symmetric fission events. From Ref. [24]. (c) The same plot as (a) except the points represent the measured data for the $^{132}\mathrm{Sn} + {}^{96}\mathrm{Zr}$ reaction with gates applied to isolate the symmetric fission events.

Figure 1 of Ref. [24]). In a previous experiment, we measured the capture-fission cross sections for the near symmetric reactions between the massive nuclei ^{124}Sn and ^{96}Zr for center-of-mass energies from 195 to 265 MeV [24]. The measured capture cross sections agreed quite well with calculations using the dinuclear systems (DNS) model [25]. This model also predicts a fusion barrier height for the $^{124}\mathrm{Sn} + {}^{96}\mathrm{Zr}$ reaction of 208.8 MeV [26], in stark contrast with the barrier height for this reaction of 216.3 MeV from the Bass model [6] and a barrier height of 241^{+5}_{-3} MeV deduced from the evaporation residue (ER) measurements of Sahm *et al.* (We note though that a previous measurement by the same group [27] for the closely related $^{124}\mathrm{Sn} + {}^{94}\mathrm{Zr}$ reaction gave a deduced fusion barrier height of 219.5 ± 3 MeV compared to the value of 238^{+5}_{-3} MeV deduced by Sahm *et al.* [13,14]. Thus there are considerable uncertainties in fusion barrier heights deduced from evaporation residue measurements by using statistical models to correct for the fission component of the cross section.)

In this work, we report an extension of the previous measurement of the capture-fission excitation function (for the $^{124}\mathrm{Sn} + {}^{96}\mathrm{Zr}$ reaction) to the $^{132}\mathrm{Sn} + {}^{96}\mathrm{Zr}$ reaction in an attempt to further clarify the role of fusion hindrance/enhancement in very neutron-rich fusing systems where fusion hindrance might be expected.

II. EXPERIMENT

The measurements were carried out at the Holifield Radioactive Ion Beam Facility (HRIBF) at Oak Ridge National Laboratory [28] with ^{132}Sn beams in the energy range 400–600 MeV and having intensities of the order of 4×10^5 pps. A set of microchannel plate detectors (MCPs) [29] separated by about one meter were placed ahead of target to get the timing information for the beam. An enriched ^{96}Zr (85.25%) target having a thickness of 380 μg/cm^2 was mounted in the middle of the scattering chamber.

The $^{132}\mathrm{Sn} + {}^{96}\mathrm{Zr}$ experiment was carried out using two different methods as explained in [24]. In the first method, four double-sided silicon strip detectors (DSSDs) of thickness 300–500 μm were used for the detection of fission fragments.

These detectors had an area of 5 × 5 cm^2 and provide energy, position, and time information for the detected fragments. These four silicon detectors were placed at a distance of 12.64 cm from the target covering an angular range of 20°–40° on either side of the beam. The detectors were calibrated using a ^{252}Cf source. Elastic scattering with lower beam energies was used for time of flight calibration. The use of inverse kinematics focuses the reaction products forward, with the expected full momentum transfer fission fragments having a folding angle of ∼70°–80°. An ion chamber [30], was placed behind the scattering chamber to monitor the energy and number of beam particles and the beam purity.

In the second method, an annular silicon detector was used for the detection of fission fragments. The detector had 48 concentric strips on one side and 16 pie-shaped sectors on the other side. The detector was placed at a distance of 2.9 cm away from the target at 0°. The annular segmented strip detector [31] had a nominal thickness of 300 μm, an inner radius of 11 mm, and an outer radius of 35 mm. Events were defined as coincidences between hits on the strips. The annular detector was calibrated using elastic scattering of a ^{130}Te beam from a gold target. The first setup had a calculated efficiency of 2% in detecting coincident fission events, and for the annular detector the efficiency was 7.1%. In comparing the two methods, one notes that the second method offers the advantages of higher count rates reducing the statistical uncertainty in the results, whereas the first method offers time-of-flight measurements leading to better discrimination against nonfusion events. The same setup was used for measurement of ^{124}Sn + ^{96}Zr reaction. A detailed description of that experiment and the data analysis is given in Ref. [24].

Most of the data were taken using the first setup with the individual silicon strip detectors. In this setup, the angles of the two coincident fragments (θ_1 and θ_2), their time-of-flights, and their respective energies (E_1 and E_2) allow a complete reconstruction of the binary process. The raw coincident experimental data can contain contributions from elastic scattering, inelastic scattering, and fusion-fission. To understand how these events can be separated, we show, in Fig. 1(a), a simulation of the expected coincident data for 600 MeV ^{124}Sn + ^{96}Zr, for a pair of detectors at ±30° with respect to the beam and angles representative of the real detectors (±10°). Elastic-scattering events are effectively cut out of the data by these angle cuts. Inelastic-scattering events, such as the $Q = -40$ MeV events shown, can be detected but give energy (E) vs. mass (M) correlations that are different from those of symmetric fission events. Gates can be set on the E vs. M plots to isolate the symmetric fission events [Fig. 1(b)]. In Fig. 1(c), we show the same gates but for the ^{132}Sn + ^{96}Zr reaction.

In the second part, where an annular silicon detector was used, time of flight information was not available and only gates on energy and angles were used to extract fission events. In Ref. [24], this setup was used for beam energies of $E_{\rm lab} = 500$ and 570 MeV. After publication, these data were reanalyzed primarily due to an error that was found in the detector efficiencies used. The resulting corrected capture fission excitation function for the ^{124}Sn + ^{96}Zr reaction is shown in Fig. 2. The corrected data was used in all comparisons of the data measured in this work with that of Ref. [24].

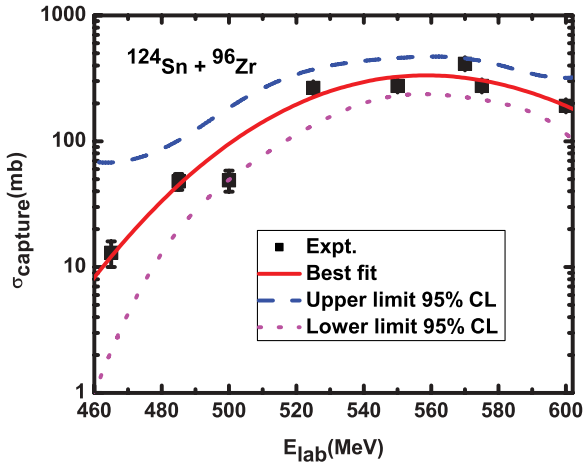

FIG. 2. (Color online) Corrected excitation function for the ^{124}Sn + ^{96}Zr reaction.

III. RESULTS AND DISCUSSION

A. Capture cross sections

In Fig. 3 we show the measured capture-fission excitation function for the ^{132}Sn + ^{96}Zr system. Also, the measured cross sections are listed in Table I. In Fig. 4, we show the previously measured [24] capture-fission cross sections for the ^{124}Sn + ^{96}Zr reaction as well as the ^{132}Sn + ^{96}Zr reaction.

In the interest of clarity, we review briefly some concepts regarding cross sections and energetics for these reactions before discussing the results. For reactions involving massive nuclei, such as the one studied in this work, the capture cross

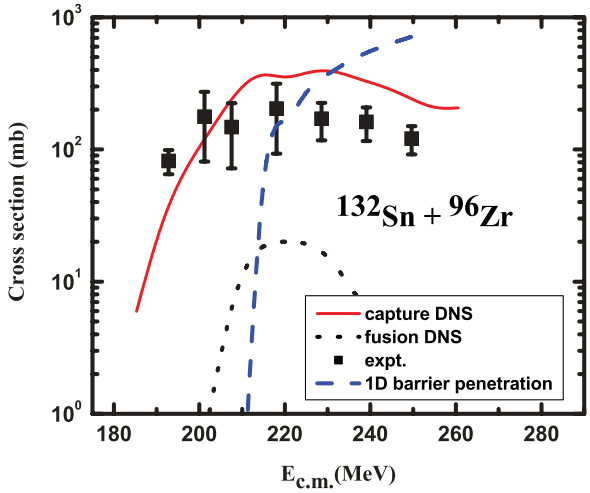

FIG. 3. (Color online) Excitation function for ^{132}Sn + ^{96}Zr capture-fission reaction. The one-dimensional barrier penetration model prediction is shown as a dashed line. The predicted capture and fusion cross sections predicted by the DNS model [25] are shown by solid and dotted lines, respectively. See text for details.

TABLE I. The measured capture reaction cross sections for ^{132}Sn + ^{96}Zr. The errors are purely statistical.

$E_{c.m.}$ (MeV)	σ(mb)	$E_{c.m.}$ (MeV)	σ(mb)
193	82 ± 17	229	171 ± 54
201	177 ± 96	239	162 ± 46
208	148 ± 76	250	121 ± 29
218	204 ± 111		

section, $\sigma_{capture}$, can be expressed as

$$\sigma_{capture} = \sigma_{ER} + \sigma_{QF} + \sigma_{FF}, \quad (1)$$

where σ_{ER}, σ_{QF}, and σ_{FF} are the evaporation residue cross section, the quasifission cross section, and the fusion-fission cross section. In lighter systems, where fission and quasifission are negligible, we have

$$\sigma_{capture} = \sigma_{ER} = \sigma_{fusion}. \quad (2)$$

In reactions forming heavy nuclei like the ^{132}Sn + ^{96}Zr → ^{228}Th reaction, the survival probability of the evaporation residues is small, and thus $\sigma_{ER} \sim \mu$b, whereas $\sigma_{capture}$ is ∼10–300 mb. Thus we will neglect σ_{ER} in our discussions and we have

$$\sigma_{capture} = \sigma_{QF} + \sigma_{FF} = \sigma_{QF} + \sigma_{fusion}. \quad (3)$$

It is difficult, but not impossible, to separate fusion-fission events from quasifission events by means of the observed mass and angular distributions [32–34]. However, with the current generation of radioactive beam facilities, the experimental uncertainties in separating quasifission and fusion-fission events due to statistical uncertainties related to the lower beam intensities do not permit meaningful separations of these components for reactions induced by radioactive beams.

For the reactions studied in this work, we can identify certain characteristic energies, such as the interaction barrier, B_{int}, the energy required to bring the colliding nuclei into contact; the fusion barrier, B_{fusion}, the energy required to bring the colliding nuclei inside the fission saddle point; the thresholds for various evaporation residue channels, such as the threshold for the 1n out reaction, the 2n out reaction, etc., and the "extra-push" energy (more formally the "extra-extra push energy" [12]), the energy required to drive the system of the colliding nuclei from the contact configuration inside the fission saddle point. We also note the "Bass barrier," a summary of a semiempirical compilation [6] of fusion barrier heights for reactions involving lighter nuclei. The frequently used calculations for treating collisions of this character are coupled-channels calculations that are calculations of the "barrier-crossing" cross section, i.e., the capture cross section. (In systems with no fusion hindrance, the capture cross section is the fusion cross section, so the barriers deduced in such calculations are taken to be fusion barriers.)

As with the previous measurements of the ^{124}Sn + ^{96}Zr reaction [24], attempts to describe the assumed capture excitation function with a simple one-dimensional barrier calculation are not successful. A one-dimensional barrier penetration calculation model calculation is shown in Fig. 3 as dashed blue line. The parameters used for the potential in this calculation are those used in the coupled-channels calculation (see below) assuming a surface diffuseness parameter of 0.63 fm and assuming "no coupling." For above-barrier energies in the ^{132}Sn + ^{96}Zr reaction, the capture cross section is significantly less than that predicted by the one-dimensional barrier penetration model, as observed for the ^{124}Sn + ^{96}Zr reaction. Also there is an enhancement for below-barrier energies compared to the one-dimensional model. In some reactions involving unstable nuclei, this situation is the result of projectile breakup. However, given the relative stability of the projectile and target nuclei, that possibility does not seem likely in this case.

The results of a coupled-channels calculation [35] are shown in Figs. 5 and 6. Along with the measured cross sections, we show two different coupled-channels calculations, one with the diffuseness parameter, a, set at its "customary value" of

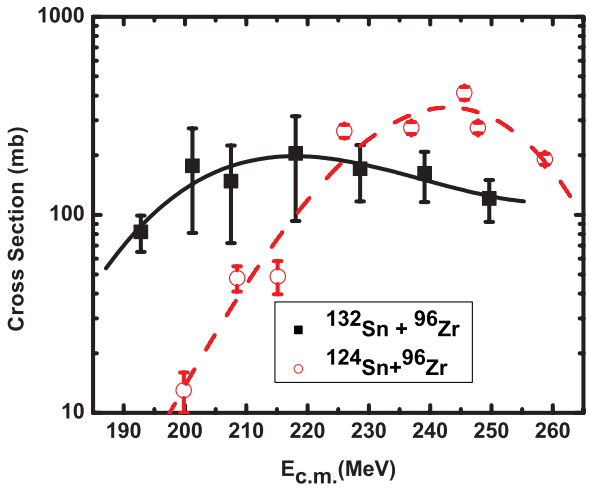

FIG. 4. (Color online) Comparison of the capture fission excitation functions for the ^{132}Sn + ^{96}Zr (solid squares and line) and ^{124}Sn + ^{96}Zr reactions (open circles and dashed line). The lines are to guide the eye through the data points. See text for details.

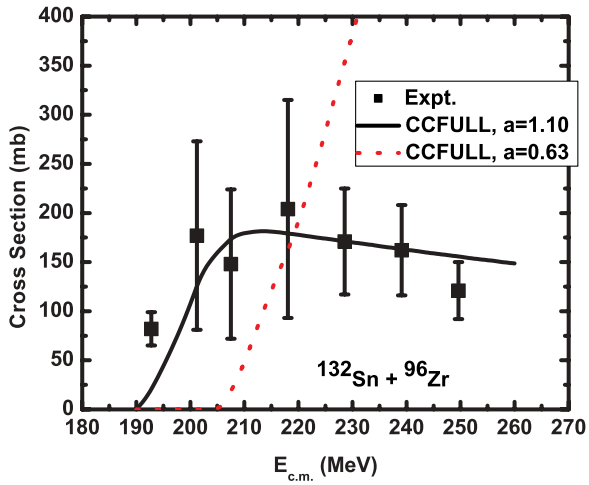

FIG. 5. (Color online) Comparison of the measured and calculated capture fission excitation functions for the ^{132}Sn + ^{96}Zr reaction. See text for details.

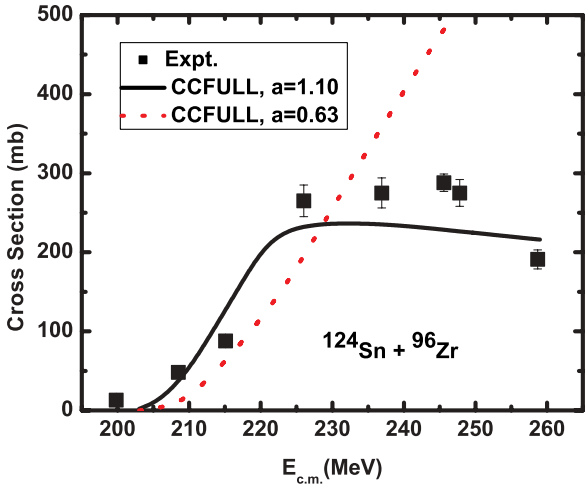

FIG. 6. (Color online) Comparison of the measured and calculated capture fission excitation functions for the ^{124}Sn + ^{96}Zr reaction.

0.63 fm and the other with a larger value of this parameter of 1.10 fm. In the calculations for the ^{132}Sn + ^{96}Zr reaction, the form of the nuclear potential was taken to be of a Woods-Saxon type with $V_0 = 125$ (MeV), $r_0 = 1.18$ (fm). The 2^+ and 3^- inelastic excitations of the target ($E_{2+} = 1.751$ MeV and $E_{3-} = 1.897$ MeV, deformation $\beta_2 = 0.08$, $\beta_3 = 0.27$ [36,37]), and no excitations of the projectile were allowed. For the ^{124}Sn + ^{96}Zr reaction, the nuclear potential was taken to be $V_0 = 108$ (MeV), $r_0 = 1.18$ (fm) with inclusion of the same excitations of the target nucleus but also including excitations of the projectile ($E_{2+} = 1.132$ MeV and and $E_{3-} = 2.614$ MeV, deformation $\beta_2 = 0.122$, $\beta_3 = 0.1532$ [38,39]). The values of the nuclear potential V_0 used in these calculations were adjusted to produce the best fit to the data. Neutron transfer channels were neglected in the calculation because they have negative Q values and thus do not play a role in this reaction. The deduced barrier parameters for the ^{132}Sn + ^{96}Zr reaction are $V_b = 192.2$ MeV, $R_b = 12.9$ fm, and $\hbar\omega = 1.7$ MeV, whereas for the ^{124}Sn + ^{96}Zr reaction, the deduced barrier parameters are $V_b = 203.5$ MeV, $R_b = 12.5$ fm, and $\hbar\omega = 2.0$ MeV. The deduced capture barriers thus differ significantly from those suggested by a recent semiempirical prescription [40] of interaction barriers of 206.8 and 209.1 MeV. In going from the ^{124}Sn + ^{96}Zr reaction to the ^{132}Sn + ^{96}Zr reaction, the deduced interaction barrier shifts downward by 11.3 MeV.

The need for a large value of the surface diffuseness parameter, a, to fit data for heavy systems has been noted before as well as its correlation with neutron-richness [41–43]. (The value of a needed in this work to fit the data is less than the predicted value of $a = 1.5$ from the systematics of this parameter [42,43].) Suggestions to explain this effect include departure of the real nuclear potential from the Woods-Saxon form or as being the result of the occurrence of fusion hindrance.

The deduced interaction barrier heights in this work are compared to other estimates of this quantity in Table II. Neither of the semiempirical estimates [6,44] correctly reproduces the magnitude of the interaction barrier height or the change in barrier height with increasing neutron-richness of the reacting system. A semiempirical correlation [2] of interaction barrier heights with $(N - Z)^2/A$ also underestimates the observed lowering.

TABLE II. Comparison of various estimates of the interaction barrier heights.

Reaction	Expt'l. (CC)	DNS (MeV)	Swiatecki *et al.* [44]
^{132}Sn + ^{96}Zr	192.2	192.3	214.8
^{124}Sn + ^{96}Zr	203.5	204.4	217.8

B. Speculations about fusion barriers

As stated earlier, we have measured capture cross sections in this work. The direct measurement of fusion cross sections requires the separation of the quasifission and fusion-fission components of the capture cross sections, which is not feasible with the current generation of radioactive beam facilities. However, for many purposes, such as heavy element syntheses, we need to know the properties of the fusion cross sections in these collisions. What should we do?

One solution to this problem is to measure evaporation residue cross sections, which is difficult given the microbarn cross sections for these reactions, and deconvolute from them, by means of a statistical model calculation, the de-excitation processes leading to evaporation residue formation and thus the fusion cross sections (10–100 mb). The statistical model must be capable of meaningfully extrapolating microbarn cross sections to millibarn cross sections, a difficult task as shown by the disagreements between such deductions by the same group [13,14,27] using different statistical models for the ^{124}Sn + ^{94}Zr reaction.

We have chosen another alternative to make this extrapolation to the fusion cross sections, i.e., to extrapolate from the capture cross sections to the fusion cross sections, which, at least, involves cross sections of similar magnitude. We do this extrapolation using the dinuclear system model. The DNS model [45–47] treats the evaporation residue production as a three-stage process. A molecule-like dinuclear system is formed after overcoming the interaction barrier in the first stage. The transformation of the DNS into a more compact compound nucleus (CN) in competition with quasifission takes place in the second stage. In the third phase, emission of neutrons and charged particles cools the CN. This model was successful in reproducing evaporation residue cross sections for ^{16}O + ^{204}Pb and ^{124}Sn + ^{96}Zr systems [45].

Calculations by Giardina *et al.* [25] using the DNS model for capture cross sections in the ^{132}Sn + ^{96}Zr reaction are shown in Fig. 3 as a solid red line. The predictions of this model for the fusion cross sections for this reaction are shown as a dotted line. Because the DNS model calculations agree reasonably well with the observed capture cross sections for the ^{132}Sn + ^{96}Zr and ^{124}Sn + ^{96}Zr reactions [24] and the evaporation residue cross sections [13,14] for the ^{124}Sn + ^{96}Zr reaction, it is reasonable to speculate that the interaction and fusion barrier heights for these reactions are those predicted

by the DNS model. For the ^{132}Sn + ^{96}Zr reaction, the deduced (DNS) interaction barrier height is 192.3 MeV, whereas the fusion barrier height is 201.8 MeV. Similarly, for the ^{124}Sn + ^{96}Zr reaction [24], the deduced interaction barrier height is 204.4 MeV, whereas the fusion barrier height is 208.9 MeV. (The values of these barrier heights are deduced from the calculations by a $1/E$ plot of those portions of the data that depend linearly on $1/E$.) The Bass barrier heights for these reactions are 213.8 and 216.3 MeV, respectively.

One immediately comes to several conclusions. The deduced fusion barrier heights from the DNS model for the reactions induced by neutron-rich radioactive beams (201.8 and 208.9 MeV) are substantially below the Bass barrier heights. A similar trend has been observed for the fusion barrier heights, deduced by an analysis of quasi–elastic scattering, for reactions leading to the synthesis of the heaviest elements with *n*-rich stable beams [48]. We take the definition that "extra-push" energy is the difference between the interaction barrier height and the fusion barrier height. This definition of the extra push energy is consistent with the original work of Swiatecki and Bjørnholm and Swiatecki [12,23]. Both the ^{124}Sn + ^{96}Zr and ^{132}Sn + ^{96}Zr reactions show positive extra push energies (fusion hindrance) of 4.5 and 9.5 MeV, respectively, as deduced from the DNS model. (Refs. [12,23] would have estimated these energies as 10 and 7 MeV, respectively). Some but not all of the advantage of using neutron-rich radioactive beams is predicted by the DNS model to be lost due to fusion hindrance in the Sn + Zr system.

IV. CONCLUSION

The capture-fission cross section for the ^{132}Sn + ^{96}Zr system was measured and compared with ^{124}Sn + ^{96}Zr system. The interaction barrier heights for these systems decrease with increasing neutron-richness of the projectile. Coupled-channels calculations can describe the data if the surface diffuseness parameter, a, is allowed to be 1.10 fm, instead of the customary 0.6 fm. The fusion hindrance, as deduced from the DNS model, is greater for the more neutron-rich system, lessening the advantage of using neutron-rich projectiles.

ACKNOWLEDGMENTS

We thank Giardina, Mandaglio, and Nasirov for furnishing the results of their calculations prior to their publication. This work was supported in part by the Director, Office of Energy Research, Division of Nuclear Physics of the Office of High Energy and Nuclear Physics of the US Department of Energy under grant DE-FG06-97ER41026 and contract no. W31-109-ENG-38 and by the National Science Foundation under NSF grant no. PHY03-54828.

[1] K. E. Zyromski, W. Loveland, G. A. Souliotis, D. J. Morrissey, C. F. Powell, O. Batenkov, K. Aleklett, R. Yanez, and I. Forsberg, Phys. Rev. C **63**, 024615 (2001).
[2] W. Loveland, D. Peterson, A. M. Vinodkumar, P. H. Sprunger, D. Shapira, J. F. Liang, G. A. Souliotis, D. J. Morrissey, and P. Lofy, Phys. Rev. C **74**, 044607 (2006).
[3] Y. X. Watanabe *et al.*, Eur. Phys. J. A **10**, 373 (2001).
[4] J. F. Liang *et al.*, Phys. Rev. C **75**, 054607 (2007).
[5] D. Shapira, Nucl. Phys. **A787**, 184c (2007).
[6] R. Bass, Nucl. Phys. **A231**, 45 (1974).
[7] D. J. Hinde, M. Dasgupta, N. Herrald, R. G. Neilson, J. O. Newton, and M. A. Lane, Phys. Rev. C **75**, 054603 (2007).
[8] P. H. Stelson, Phys. Lett. **B205**, 190 (1988).
[9] P. H. Stelson, H. J. Kim, M. Beckerman, D. Shapira, and R. L. Robinson, Phys. Rev. C **41**, 1584 (1990).
[10] V. I. Zagrebaev, Phys. Rev. C **67**, 061601(R) (2003).
[11] K. E. Rehm, Annu. Rev. Nucl. Part. Sci. **41**, 429 (1991).
[12] S. Bjørnholm and W. J. Swiatecki, Nucl. Phys. **A391**, 471 (1982).
[13] C. C. Sahm *et al.*, Z. Phys. A **319**, 113 (1984).
[14] C.-C. Sahm, H.-G. Clerc, K.-H. Schmidt, W. Reisdorf, P. Armbruster, F. P. Hessberger, J. G. Keller, G. Munzenberg, and D. Vermeulen, Nucl. Phys. **A441**, 316 (1985).
[15] A. B. Quint *et al.*, Z. Phys. A **346**, 119 (1993).
[16] W. Reisdorf *et al.*, Phys. Rev. Lett. **49**, 1811 (1982).
[17] W. Reisdorf, J. Phys. G: Nucl. Part. Phys. **20**, 1297 (1994).
[18] H. Ernst, W. Henning, C. N. Davids, W. S. Freeman, T. J. Humanic, F. W. Prosser, and R. A. Racca, Phys. Rev. C **29**, 464 (1984).
[19] K. T. Lesko, W. Henning, K. E. Rehm, G. Rosner, J. P. Schiffer, G. S. F. Stephans, B. Zeidman, and W. S. Freeman, Phys. Rev. C **34**, 2155 (1986).
[20] K.-H. Schmidt and W. Morawek, Rep. Prog. Phys. **54**, 949 (1991).
[21] H.-G. Clerc, J. G. Keller, C.-C. Sahm, K.-H. Schmidt, H. Schulte, and D. Vermeulen, Nucl. Phys. **A419**, 571 (1984).
[22] J. G. Keller, K.-H. Schmidt, H. Stelzer, W. Reisdorf, Y. K. Agarwal, F. P. Hessberger, G. Munzenberg, H. G. Clerc, and C. C. Sahm, Phys. Rev. C **29**, 1569 (1984).
[23] W. J. Swiatecki, Phys. Scr. **24**, 113 (1981); Nucl. Phys. **A376**, 275 (1982).
[24] A. M. Vinodkumar, W. Loveland, P. H. Sprunger, D. Peterson, J. F. Liang, D. Shapira, R. L. Varner, C. J. Gross, and J. J. Kolata, Phys. Rev. C **74**, 064612 (2006).
[25] G. Giardina, G. Mandaglio, and A. K. Nasirov (private communication, 2006).
[26] The value of the fusion barrier height of 208.8 MeV is different than that quoted in Ref. [24] of 208.0 MeV and reflects a re-evaluation of the data.
[27] K. H. Schmidt *et al.*, Z. Phys. A **301**, 21 (1981).
[28] J. D. Garrett, Nucl. Phys. **A616**, 3c (1997).
[29] D. Shapira and T. A. Lewis, in *Proceedings of the 17th Conference on Application of Accelerators in Research and Industry*, edited by J. L. Duggan and I. L. Morgan (AIP, New York, 2003), p. 545.
[30] D. Shapira, J. F. Liang, C. J. Gross, R. L. Varner, H. Amro, C. Harlin, J. J. Kolata, and S. Novotny, Nucl. Instr. Meth. A **551**, 330 (2005).
[31] Micron Semiconductor Ltd., Model No. S2.
[32] B. B. Back, Phys. Rev. C **31**, 2104 (1985).

[33] M. G. Itkis *et al*., Nucl. Phys. **A787**, 150c (2007).
[34] R. S. Naik, W. Loveland, P. H. Sprunger, A. M. Vinodkumar, D. Peterson, C. L. Jiang, S. Zhu, X. Tang, E. F. Moore, and P. Chowdhury, Phys. Rev. C **76**, 054604 (2007).
[35] K. Hagino, N. Rowley, and A. T. Kruppa, Comput. Phys. Commun. **123**, 143 (1999).
[36] S. Raman, C. W. Nestor, Jr., S. Kahane, and K. H. Blatt, At. Data Nucl. Data Tables **42**, 1 (1989).
[37] R. H. Spear, At. Data Nucl. Data Tables **42**, 55 (1989).
[38] J. Bryssinck *et al*., Phys. Rev. C **59**, 1930 (1999).
[39] J. Bryssinck *et al*., Phys. Rev. C **61**, 024309 (2000).
[40] K. Siwek-Wilczynska and J. Wilczynski, Phys. Rev. C **69**, 024611 (2004).
[41] K. Hagino, N. Rowley, T. Ohtsuki, M. Dasgupta, J. O. Newton, and D. J. Hinde, AIP Conference Proceedings, in *Tours Symposium on Nuclear Physics V*, edited by M. Arnould *et al*., Vol. 704, 82 (2004).
[42] J. O. Newton, C. R. Morton, M. Dasgupta, J. R. Leigh, J. C. Mein, D. J. Hinde, H. Timmers, and K. Hagino, Phys. Rev. C **64**, 064608 (2001).
[43] J. O. Newton, R. D. Butt, M. Dasgupta, D. J. Hinde, I. I. Gontchar, C. R. Morton, and K. Hagino, Phys. Lett. **B586**, 219 (2004).
[44] W. J. Swiatecki, K. Siwek-Wilczynska, and J. Wilczynski, Phys. Rev. C **71**, 014602 (2005).
[45] G. Fazio, G. Giardina, A. Lamberto, A. I. Muminov, A. K. Nasirov, F. Hanappe, and L. Stuttge, Eur. Phys. J. A **22**, 75 (2004).
[46] G. Fazio, G. Giardina *et al*., Phys. Rev. C **72**, 064614 (2005).
[47] G. Fazio, G. Giardina *et al*., Mod. Phys. Lett. A **20**, 391 (2005).
[48] S. Mitsuoka, H. Ikezoe, K. Nishio, K. Tsuruta, S. C. Jeong, and Y. Watanabe, Phys. Rev. Lett. **99**, 182701 (2007).